EUROPEAN ORGANIZATION FOR NUCLEAR RESEARCH
European Laboratory for Particle Physics

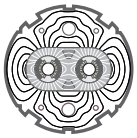

Large Hadron Collider Project

LHC Project Report 411

CORRECTION SCHEMES FOR THE NORMAL OCTUPOLE AND DECAPOLE ERRORS IN THE LHC DIPOLES

Y. Papaphilippou, BNL, Upton NY 11973, USA
e-mail: papap@bnl.gov

Abstract

Different correction schemes for curing the effect of the normal octupole and decapole multipole errors of the LHC main dipoles, at injection, are investigated. Frequency and diffusion maps are constructed and compared for two working points and for different values of the momentum deviation. The excitation of individual resonant driving terms is estimated through high order normal form construction techniques. The resonance analysis results are finally verified through short-term element by element tracking.

Extended version of a paper presented at EPAC2000, 26-30 June 2000, Vienna, Austria

Administrative Secretariat
LHC Division
CERN
CH-1211 Geneva 23
Switzerland

Geneva, 15 August 2000

1 Correction Schemes

The main limitation for the stability of the LHC [1] beam at the injection energy of 450 GeV is the magnet imperfections in the 1104 super-conducting arc (main) dipoles which introduce non-linear transverse fields expressed in the usual complex multipole expansion:

$$B_y + i\,B_x = B_1 \sum_{n=1}^{\infty} (b_n + i a_n) \left(\frac{x + i\,y}{R_r} \right)^{n-1} \quad , \tag{1}$$

where B_x, B_y are the horizontal and vertical components of the magnetic field with the normal (or erect) b_n and skew a_n multipole coefficients, B_1 is the magnetic dipole field in the vertical y direction and $R_r = 17$mm the reference radius. The multi-polar components responsible for the perturbations from the ideal dipole field are due to the persistent currents in the filaments of the super-conductor, the design geometry and the fabrication tolerances. Taking into account all the previous effects, error tables are estimated and used for beam dynamics analysis. The most important errors allowed by the dipole symmetry are the normal sextupole b_3 and decapole b_5. The normal octupole b_4 has a non-negligible effect due to the geometric imperfections induced by the two-in-one form of the LHC dipoles. The normal sextupole, octupole and decapole coefficients corresponding to the 9901 error table are displayed in Table 1. The dominant normal sextupole error is planned to be corrected by magnetic coils (spool pieces) placed at the entrance of each dipole and powered in series in each arc, in order to cancel locally the systematic effect. The same strategy can also be followed for the octupole and decapole, where the correction is done with a spool piece having both components.

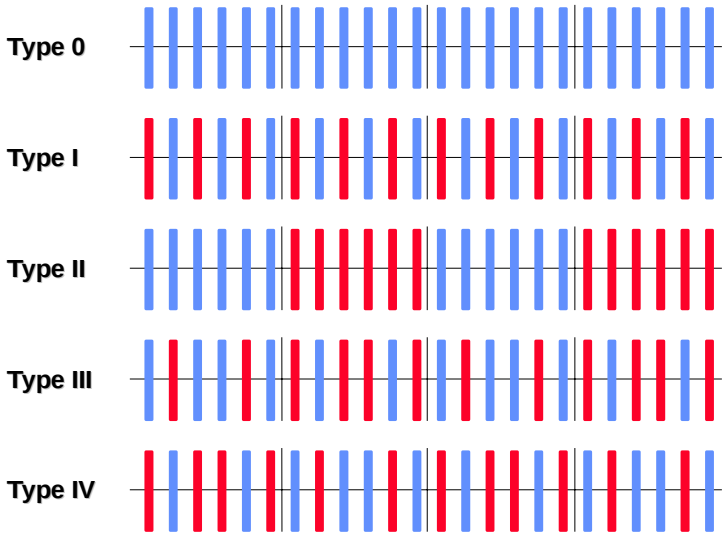

Figure 1: Representation of five different correction schemes in four cells of the LHC. The dipoles with and without octupole/decapole corrector are shown in blue and red, respectively.

Previous studies for the erect octupole [2] and decapole [3] correction have shown that the dynamic aperture of the LHC at injection could be preserved even if half of the correctors are used. In order to validate these results for LHC optics version 6, the following correction schemes have been considered [4] :

- Type O: Correctors at all dipoles in all arcs; this is the reference case.
- Type I: Correctors in every second dipole; this is a scheme proposed for the SSC and it is an interesting option for the LHC as it minimizes the electrical noise in the power converters [5].

– Type II: Correctors in every second cell; it is a proposed layout worked out to balance the inductance on the bus-bars [5].
– Type III: Correctors in every second dipole with a swap of the two types of dipoles every half-cell; this arrangement should also be better than the reference case with respect to electrical noise.
– Type IV: Same as Type III but the two types of dipoles are inverted.

Table 1: Erect sextupole, octupole and decapole field errors in the LHC dipoles (error table 9901), for a reference radius of $R_r = 17$mm in units of 10^{-4} of the main field.

Error	Systematic	Random
b_3	-8.32	1.47
b_4	0.57	0.51
b_5	1.32	0.43

A graphical representation of the correction schemes can be found in Fig. 1, where we represent the dipoles with and without octupole/decapole correctors in four cells of the LHC arc (the quadrupoles are omitted).

In this paper we present the studies undertaken for the dynamic analysis of the different correction schemes. Frequency and diffusion maps [6] were constructed for comparing their impact on non-linear dynamics. In order to check the efficiency of each scheme on resonance compensation, the resonance driving terms are computed, through high-order perturbation theory methods [7] and numerical post-processors [8]. Finally, the resonance analysis results are verified through 1000-turns element by element tracking.

2 Frequency Maps

The machine considered was LHC optics version 6 with the integer tune split of four $(63, 59)$. The LHC model constructed with MAD [9] includes systematic plus 1σ random errors in all the dipoles and can be considered as a worst case scenario. The normal sextupole error on the main dipoles has been corrected with spool pieces in every dipole around the machine and connected in series in each arc such as to eliminate the systematic component. Short-term tracking was performed with SIXTRACK [10] for two different working points: the nominal one $(Q_x, Q_y) = (0.28, 0.31)$ and another interesting candidate for the LHC operation $(Q_x, Q_y) = (0.21, 0.24)$ which has the same split between the tunes and the same distance to the tune space diagonal. This working point is closer to the 5th order resonance $(5, 0)$ on the horizontal plane and the 4th order $(4, 0)$ on the vertical plane.

Apart from the 4D cases ($\delta p/p = 0$), it was also essential to perform tracking with a constant momentum deviation $\delta p/p = 7.5 \times 10^{-4}$, at approximately 75% of the full bucket size. As off-momentum particles cross areas where the dispersion is non-zero (typically 1-2m in the LHC arc), feed-down effects are generated by the multipoles: to first order in the dispersion function, the decapole will create an octupole, the octupole will create a sextupole, etc. The octupole produces a first order tune-shift, which is linear with the transverse emittance. The decapole has a second order contribution (quadratic in the decapole strength and in the emittances). On the other hand, for off-momentum particles, the decapole gives an octupole feed-down and thus contributes to a first order tune-shift. The total first order "octupole-like"

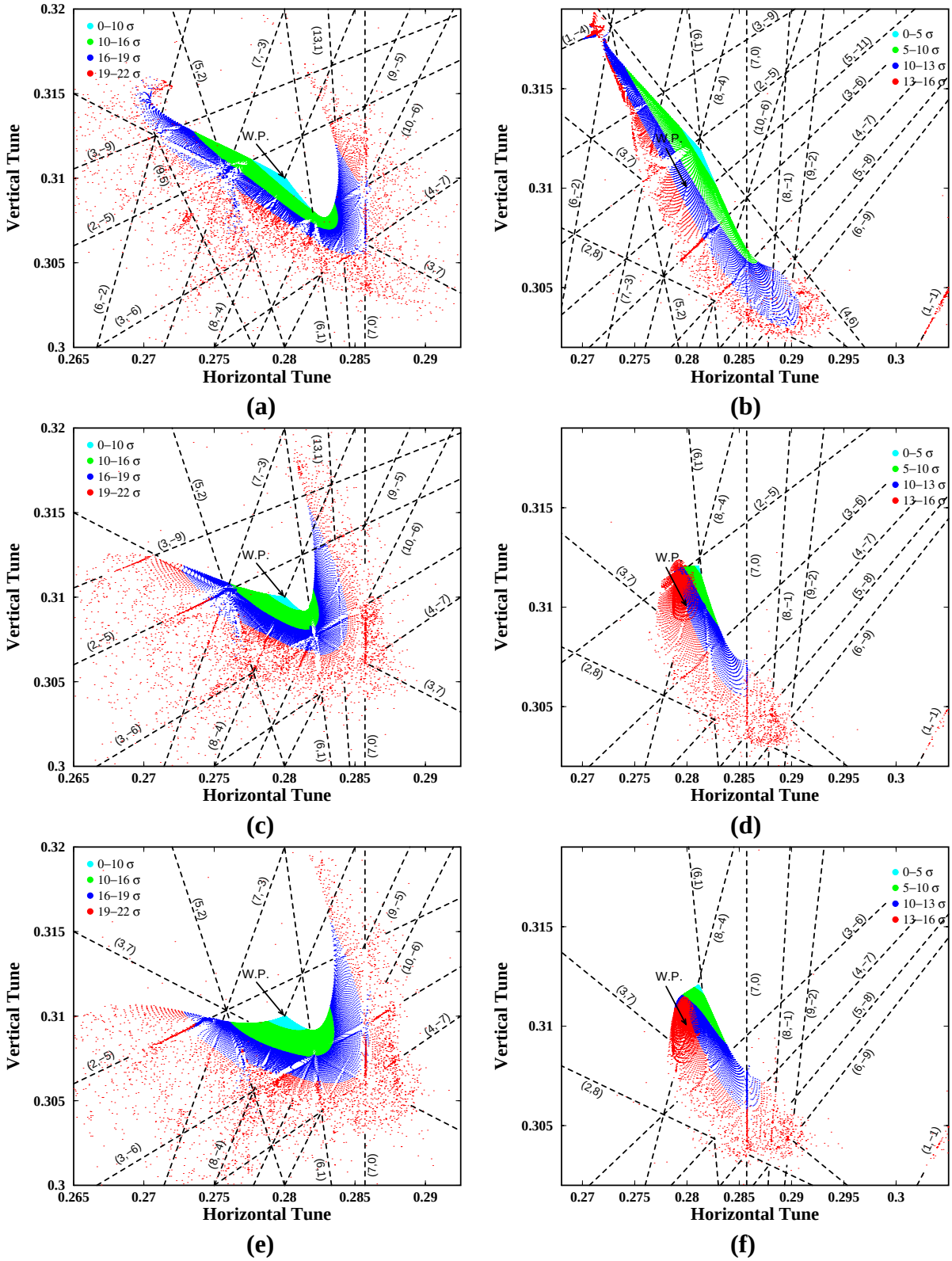

Figure 2: Frequency maps when the octupole and decapole components are not corrected, (top) with correctors in all dipoles (middle), and with correctors in every second dipole (bottom) for two different momentum spreads $\delta p/p = 0$ (left) and $\delta p/p = 7 \times 10^{-4}$ (right), and for the nominal working point $(Q_x, Qy) = (0.28, 0.31)$.

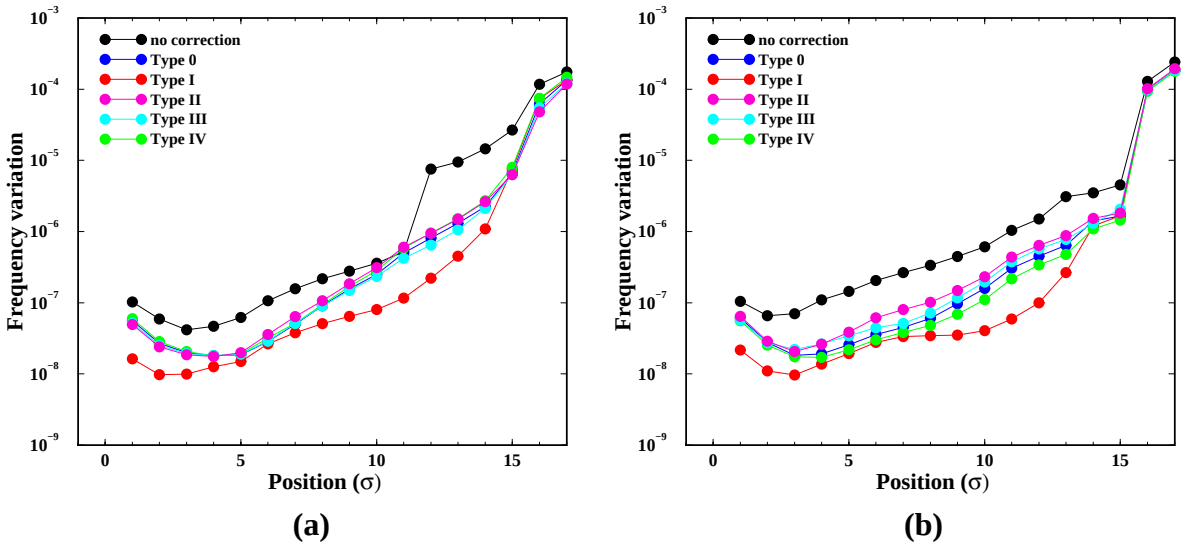

Figure 3: Evolution of the frequency variation averaged over all directions, with the particles' amplitude (in σ) for $\delta p/p = 7 \times 10^{-4}$, and for two different tunes (a) $(Q_x, Qy) = (0.28, 0.31)$ and (b) $(Q_x, Qy) = (0.21, 0.24)$.

detuning given by k localized thin element kicks is

$$\delta\nu_{x,y} = \frac{3}{2\pi\rho}\sum_k \left(\frac{b_{4k}}{4} + b_{5k}D_{xk}\frac{\delta p}{p}\right)\beta_{x,y_k}\left(\beta_{x,y_k}J_{x,y} - 2\beta_{y,x_k}J_{y,x}\right) \quad , \tag{2}$$

where D_{xk} is the horizontal dispersion (the vertical dispersion is considered to be zero as in the LHC arc). Using the values of Table 1, we may have a crude estimate of the contribution to the detuning due to the decapole feed-down for off-momentum particles: it is around 1 % of the effect of the normal octupole.

Frequency maps [6] were produced for all the correction cases. As an example, we present in Fig. 2, six maps issued by 4D (left) and 5D (right) tracking of 10000 particles for the nominal working point $(Q_x, Q_y) = (0.28, 0.31)$ and two different models: the non-corrected case (top) the reference correction (middle) and the one having the correctors placed in every second dipole (bottom). The different colors in the maps represent different amplitude windows, up to 22 and 16 σ for the 4D and 5D case, respectively. As expected, the non-corrected case is very bad with respect to non-linear dynamics. The tune-shift is quite large especially for particles with large vertical amplitude (left corner of the plots). The most excited resonance is the normal 7th order $(2, -5)$ and the 9th order $(3, -6)$. Their interplay with other 7th order and 10th order resonances, represented as crossings of lines in the map, can perturb severely the particle motion. For the 5D case, it is important to point out that there is a shift in the tune for "zero-amplitude" particles which is caused by the fact that the chromaticity is not zero (actually it is equal to -2). In that case, the particles are shifted up towards the normal 5th order $(1, -4)$ resonance, for the uncorrected case. Note also the trapped particles close to the diagonal (resonance $(1, -1)$). The correction seems quite efficient, as the tune-shift is reduced, especially in the off-momentum case.

For the other working point, maps were also constructed and dangerous resonances where identified. Especially the $(5, 0)$ resonance is approached by particles with high vertical amplitudes in the uncorrected case. The correction helps avoiding this resonance by reducing the detuning. For the other correction schemes the maps look quite similar. Especially the Type I

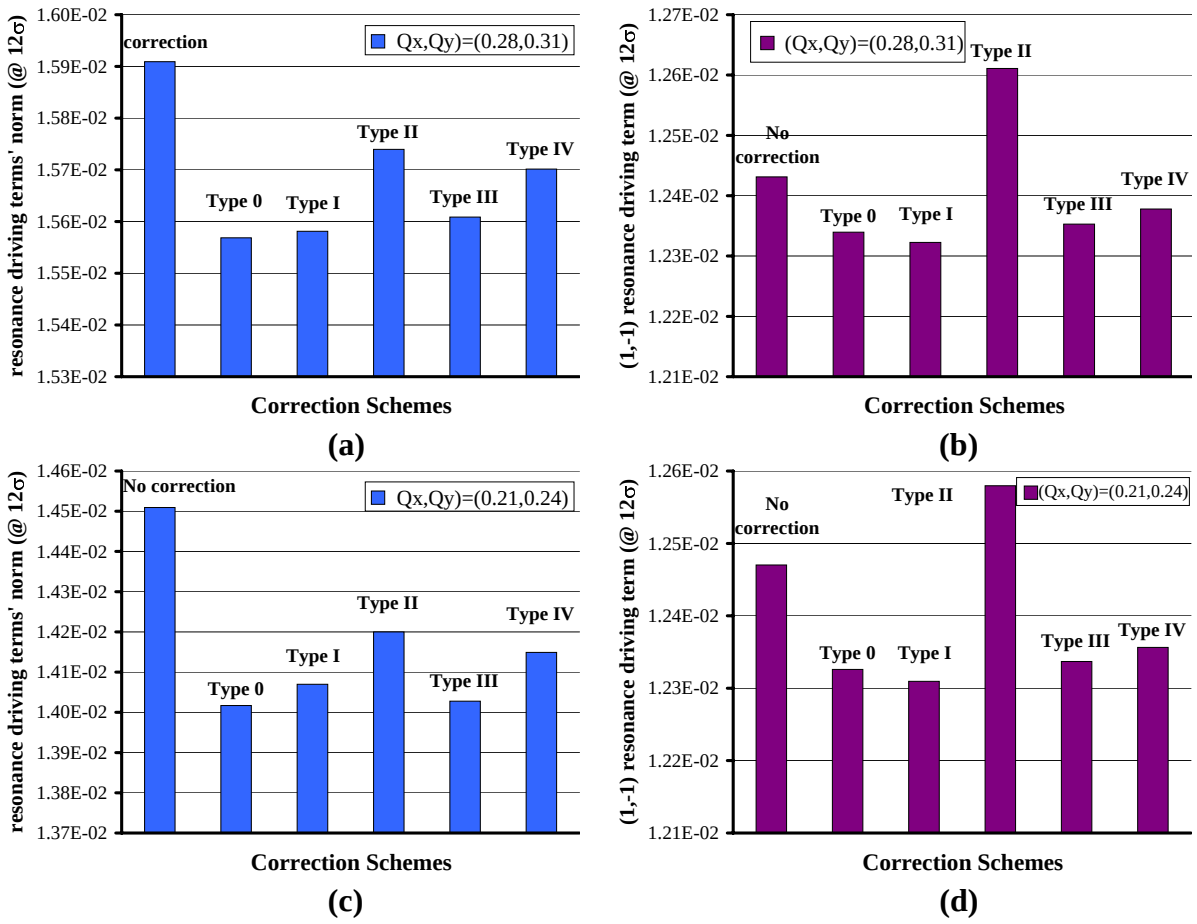

Figure 4: Resonance driving terms' norm (left) and driving term of the $(1,-1)$ resonance (right) extracted by 4D DaLie [7] maps, for two different working points $(Q_x, Qy) = (0.28, 0.31)$ and $(0.21, 0.24)$. The driving terms are evaluated at 12σ and averaged over eleven different directions of the phase space, with GRR [8].

scheme (every second dipole) is quite good, even if the detuning seems to be bigger. In that case, and for motion close to the vertical plane, the tune-shift pushes the particles away from the dangerous crossing of resonances ($(5,2)$ with $(2,-5)$ for the nominal working point and $(5,0)$ with $(1,-5)$ for the second one). In Fig. 3, we plot in logarithmic scale the frequency variation norm [6] averaged over the angles versus the amplitude, for both working points, for all correction schemes and for the non-zero momentum spread. These plots confirm that all the correction schemes are quite similar. The Type I (red dots) correction scheme seems to generate less perturbation for small amplitudes, in contrast with the Type II (every second cell - pink dots), which seems slightly worse.

3 Resonance Analysis

In order to have some more insight about the resonance excitation with respect to the different correction schemes, we constructed 11th order 4D maps [7] for every correction case and post-processed the normal form results with GRR [8], in order to compute the resonance driving terms at a specific position of the phase space. In Fig. 4, we plot the resonance driving terms' norm (the sum of squares of all resonances up to 12th order) averaged over eleven directions in the phase space and computed at an amplitude of 12 σ. We should point out that 99.9 % of the contribution comes from resonances of order 7 and below and more then 85 % comes from

the $(1,-1)$ resonance, whose phase averaged strength is also plotted in Fig. 4. There is a clear difference between the corrected and uncorrected cases, especially due to the contribution of all other resonances (left plots). On the other hand, the $(1,-1)$ resonance seems quite excited in all cases (right plots). This resonance was already identified to be one of the major dynamic aperture limitations the of LHC optics version 5, especially due to the integer tune-split of four (63,59). In particular, for the correction scheme II (every second cell), the strength of this resonance is even higher then in the uncorrected case. The change of the tune-split from four to five will most probably cure this undesirable effect. All the other correction schemes seem to have approximately the same resonance excitation, with the reference correction scheme being slightly better. A partial result from this representation is that the resonance excitation seems smaller for the working point (0.21,0.24) then for the nominal one. This can be also observed in the frequency variation (Fig. 3), where particles with the same amplitude have higher diffusion coefficient for the working point (0.28,0.31).

4 Results of Short Term Tracking

The ultimate test for backing-up the arguments and results extracted by the dynamic analysis of the correction schemes is provided by the 1000 turns dynamic aperture estimation through element by element tracking. In Fig. 5, we present the dynamic aperture results for the two working points and momentum spreads. The particles are launched in 200 different directions of the configuration space with zero velocities. The pictures display the dynamic aperture for each direction in the transverse position space (horizontal versus vertical initial amplitude) and the different colors denote different correction cases. These plots are complementary with the frequency maps, as they show the exact areas where particles are lost and can be associated with the resonance crossings shown in Figs. 2.

In these pictures, all the correction schemes seem to be equivalent. Of course, the non-corrected case has the lowest dynamic aperture (note the scattered green crosses in lower amplitudes) especially for the second working point and off-momentum particles (Fig. 5d). In that case, and for motion close to the horizontal plane, there is at least a $1-1.5\sigma$ difference between the corrected and uncorrected cases. On the other hand, as the shapes formed by the lost particles' initial conditions are almost identical, it seems that this is entirely due to the higher tune-shift in the uncorrected case. This remark stands for the other plots, as well. One may also argue that the Type II is slightly worse (scattered pink boxes in the edge of the loss zones) but the difference with the other correction schemes seems very small. Finally, in all the cases the dynamic aperture is smaller for particles launched close to the horizontal plane and off-momentum. On the other hand, the difference between vertical and horizontal space motion is quite marginal in the on-momentum cases. This should be correlated with the fact that for off-momentum cases the particles with large horizontal amplitudes are moving towards the $(1,-1)$ resonance in the bottom right corner of the frequency maps and get quickly lost, especially in the uncorrected case (see Fig 2).

We can have a clearer idea about the efficiency of the correction schemes by the survival plots displayed in Fig. 6. In these figures, the number of lost particles is displayed, over the 10000 tracked for 1000 turns, and all the studied correction schemes. It is clear from these plots that the highest number of lost particles for both working points and momentum deviations occur in the uncorrected case. Then, the correction scheme II (correctors in every second cell) is the least efficient in all cases except the one of the nominal working point and off-momentum particles. In that case, all the correction schemes are quite close with the surprisingly good performance of the Type I (correctors in every second dipole) which is generally quite efficient and close to the reference case (correctors in every dipole). Let us however point out that the

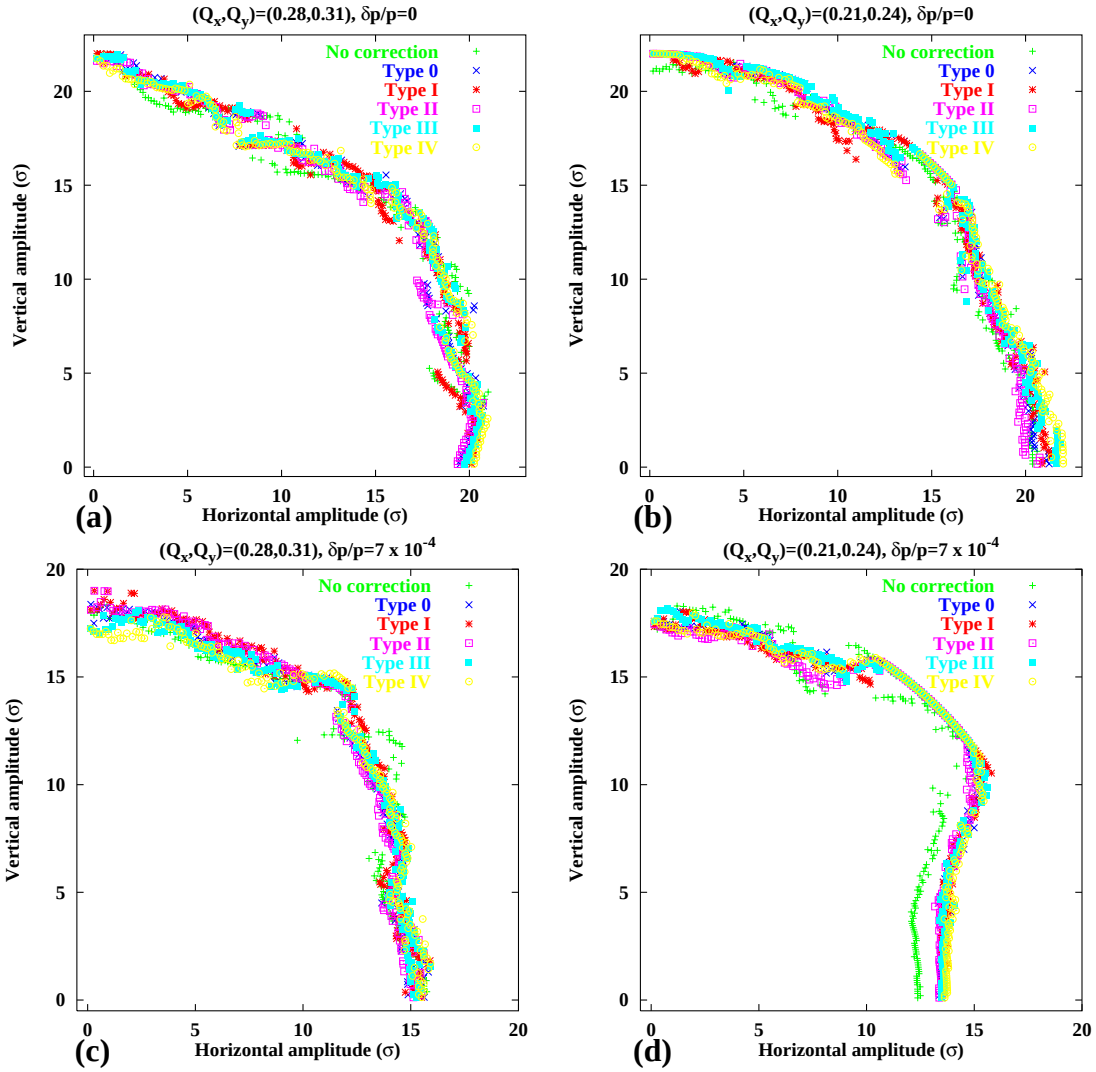

Figure 5: Loss zones in the initial conditions space for all the correction cases. The particles are launched in 200 different directions of the transverse position space with zero velocities and tracked for 1000 turns. Here are shown the results for two different working points $(Q_x, Qy) = (0.28, 0.31)$ (left) and $(0.21, 0.24)$ (right) and two different momentum spreads $\delta p/p = 0$ (top) and $\delta p/p = 7 \times 10^{-4}$ (bottom).

difference of particle losses between the correction schemes is within a 5% of the total number of tracked particles (500 over 10000), and should be considered as marginal.

The ultimate comparison of the correction schemes is done in Fig. 7, where we compare the phase space averaged (over the 200 directions) dynamic aperture for all the studied models. There is a striking correlation between these plots and the resonance excitation plots in Fig. 4. It is also interesting to observe that the dynamic aperture is slightly better in the case of the $(0.21, 0.24)$ working point when the normal octupole and decapole are corrected. On the other hand, all the correction schemes seam quite equivalent. In fact, their difference is within 0.5σ which is probably very close to the precision level of the dynamic aperture estimation. We can still confirm, however, that the Type II correction scheme is worse and that the Type I is equivalent with the reference case, and in one case (nominal working point and off-momentum tracking) gives even a higher dynamic aperture.

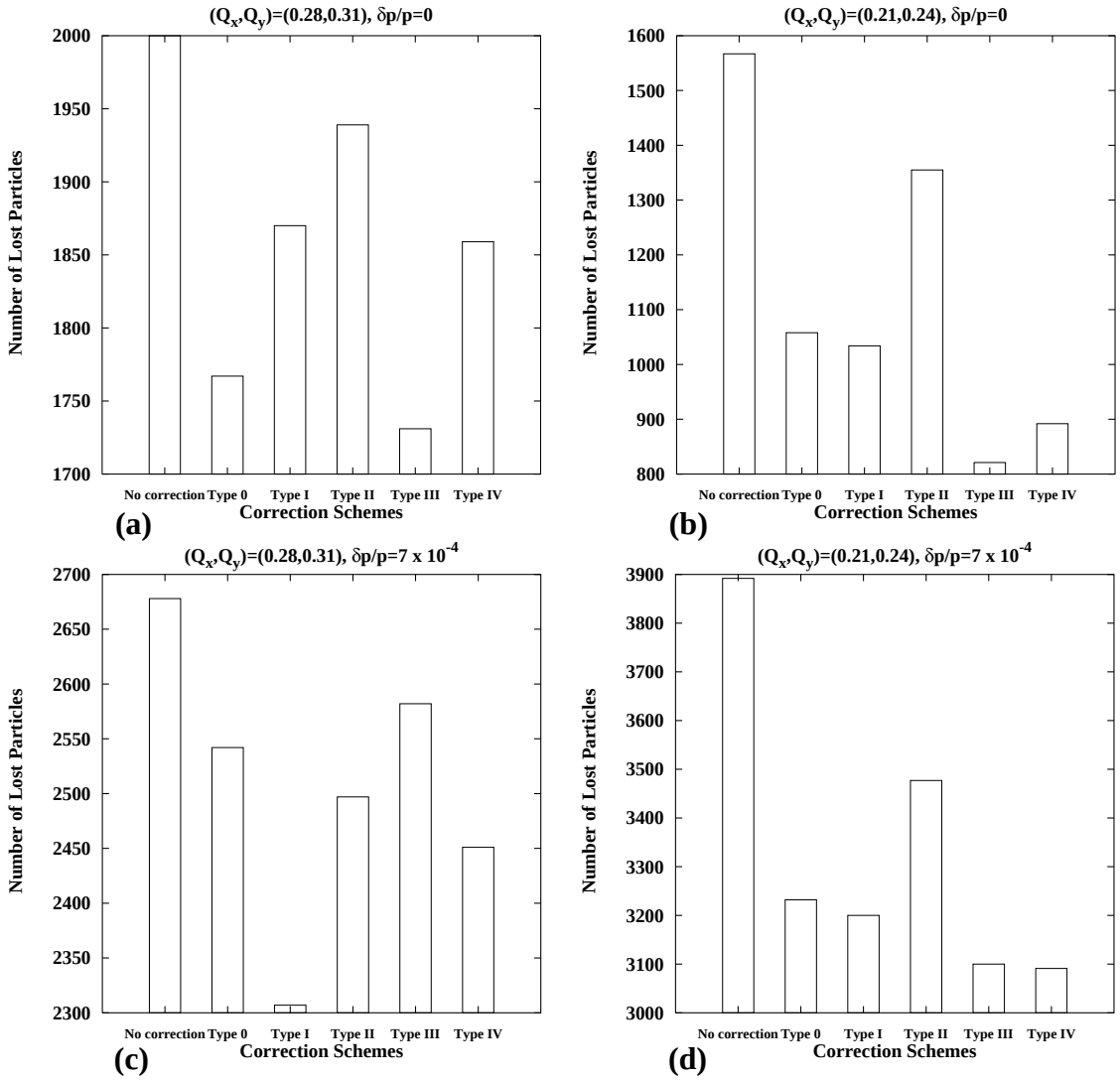

Figure 6: Number of lost particles for all the correction cases. The total number of tracked particles is 10000. Here are shown the results for two different working points $(Q_x, Qy) = (0.28, 0.31)$ (left) and $(0.21, 0.24)$ (right) and two different momentum spreads $\delta p/p = 0$ (top) and $\delta p/p = 7 \times 10^{-4}$ (bottom).

5 Conclusion

A variety of correction schemes for the erect octupole and decapole multipole errors in the LHC main dipoles have been studied and compared with respect to their impact on the non-linear dynamics of the machine, at injection. Apart from the reference correction scheme where all the dipoles had octupole/decapole correctors, all the other schemes had half of the correctors present. We showed that the different correction strategies are equivalent from the point of view of non-linear dynamics. Based on the small differences observed in dynamical parameters studied (detuning, resonance excitation, global diffusion coefficient, short term dynamic aperture) their performance can be graded as follows: the scheme for which the correctors are placed in every second cell is slightly worse and the one with the correctors placed in every dipole is slightly better, followed by the scheme where the correctors are placed in every second dipole. It is thus confirmed that by using half of the correctors will be sufficient to correct the normal octupole and decapole errors in the LHC main dipoles, even if the reference case (correctors in

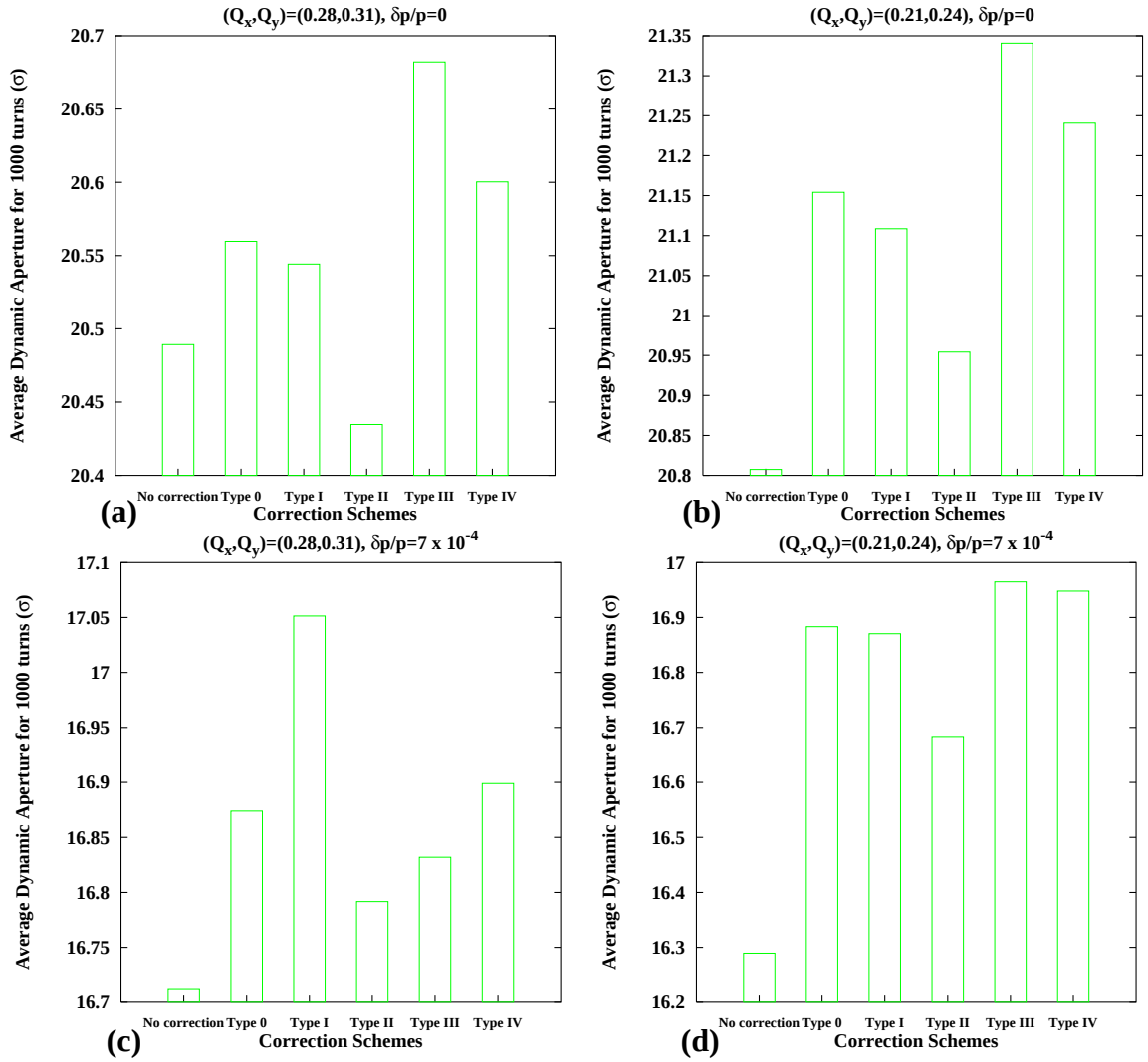

Figure 7: Average dynamic aperture for all the correction cases. The particles are launched in 200 different directions of the transverse position space with zero velocities and tracked for 1000 turns. Here are shown the results for two different working points $(Q_x, Qy) = (0.28, 0.31)$ (left) and $(0.21, 0.24)$ (right) and two different momentum spreads $\delta p/p = 0$ (top) and $\delta p/p = 7 \times 10^{-4}$ (bottom).

every one of them) is probably safer. Element by element short term tracking confirmed the resonance analysis results and especially the marginal difference between the correction schemes.

6 Acknowledgments

The author would like to thank J.-P. Koutchouk for suggesting this study, F. Ruggiero for his comments on an early version of the report and, finally, O. Bruning and L. Walckiers for discussions and remarks.

References

[1] The LHC Study Group, CERN/AC/95-05 (LHC), 1995.
[2] Y. Papaphilippou, et al., LHC Project Report 253, 1998.
[3] F. Schmidt, G. Xu, LHC Project Note 98, 1997.
[4] J.-P. Koutchouk, private communication.

[5] F. Bordry, et al., LHC Project Report 170, 1998; P. Proudlock, LHC Project Report 302, 1999.
[6] J. Laskar, Physica D 67, 257, 1993; J. Laskar, D. Robin, Part. Accel. 54, 183, 1996; Y. Papaphilippou, PAC'99, New York, 1999.
[7] M. Berz, et al., Part. Accel., 24, 91 109, 1989; Berz, M., Part. Accel., 24, 109, 1989; E. Forest, The DaLie Code, unpublished, 1986; J. Irwin, et al., EPAC'94, London, 1994.
[8] Y. Papaphilippou, F. Schmidt, AIP C.P. 468, 1999.
[9] H. Grote, F.C. Iselin, CERN/SL/90-13, 1990.
[10] F. Schmidt, CERN/SL/94-56, 1994.